Regular Article

THROMBOSIS AND HEMOSTASIS

Platelets induce apoptosis via membrane-bound FasL

Rebecca I. Schleicher,[1,2] Frank Reichenbach,[3-5] Peter Kraft,[6] Anil Kumar,[7] Mario Lescan,[8] Franziska Todt,[3] Kerstin Göbel,[9] Ingo Hilgendorf,[10] Tobias Geisler,[2] Axel Bauer,[2] Marcus Olbrich,[1,2] Martin Schaller,[11] Sebastian Wesselborg,[12] Lorraine O'Reilly,[13] Sven G. Meuth,[9] Klaus Schulze-Osthoff,[14] Meinrad Gawaz,[2] Xuri Li,[15] Christoph Kleinschnitz,[6] Frank Edlich,[3,16] and Harald F. Langer[1,2]

[1]Department of Cardiovascular Medicine, Section for Cardioimmunology, and [2]Department of Cardiovascular Medicine, University Hospital, Eberhard Karls University, Tuebingen, Germany; [3]Institute for Biochemistry and Molecular Biology, Centre for Biochemistry and Molecular Cell Research (ZBMZ), [4]Faculty of Biology, and [5]Spemann Graduate School of Biology and Medicine, University of Freiburg, Freiburg, Germany; [6]Department of Neurology, University Hospital Wuerzburg, Wuerzburg, Germany; [7]National Eye Institute, Bethesda, MD; [8]Department of Cardiovascular Surgery, University Hospital, Eberhard Karls University, Tuebingen, Germany; [9]Department of Neurology and Institute of Physiology (Neuropathophysiology), University of Muenster, Muenster, Germany; [10]Department of Cardiology and Angiology I, Heart Center, University of Freiburg, Freiburg, Germany; [11]Department of Dermatology, University Hospital, Eberhard Karls University, Tuebingen, Germany; [12]Institute for Molecular Medicine, Heinrich-Heine University Dusseldorf, Dusseldorf, Germany; [13]The Walter and Eliza Hall Institute of Medical Research, Parkville, VIC, Australia; [14]Interfaculty Institute of Biochemistry, University of Tuebingen, Tuebingen and German Cancer Consortium and German Cancer Research Center, Heidelberg, Germany; [15]State Key Laboratory of Ophthalmology, Zhongshan Ophthalmic Center, Sun Yat-Sen University, Guangzhou, Guangdong, People's Republic of China; and [16]BIOSS Centre for Biological Signalling Studies, University of Freiburg, Freiburg, Germany

Key Points

- PLTs contribute to apoptosis in vivo and express the death receptor ligand FasL upon activation.
- Membrane-bound FasL mediates PLT-induced apoptosis, whereas Bax/Bak signaling is not required but reinforces PLT-induced apoptosis.

After tissue injury, both wound sealing and apoptosis contribute to restoration of tissue integrity and functionality. Although the role of platelets (PLTs) for wound closure and induction of regenerative processes is well established, the knowledge about their contribution to apoptosis is incomplete. Here, we show that PLTs present the death receptor Fas ligand (FasL) on their surface after activation. Activated PLTs as well as the isolated membrane fraction of activated PLTs but not of resting PLTs induced apoptosis in a dose-dependent manner in primary murine neuronal cells, human neuroblastoma cells, and mouse embryonic fibroblasts. Membrane protein from PLTs lacking membrane-bound FasL ($FasL^{\triangle m/\triangle m}$) failed to induce apoptosis. Bax/Bak-mediated mitochondrial apoptosis signaling in target cells was not required for PLT-induced cell death, but increased the apoptotic response to PLT-induced Fas signaling. In vivo, PLT depletion significantly reduced apoptosis in a stroke model and an inflammation-independent model of *N*-methyl-D-aspartic acid-induced retinal apoptosis. Furthermore, experiments using PLT-specific $PF4Cre^{+}$ $FasL^{fl/fl}$ mice demonstrated a role of PLT-derived FasL for tissue apoptosis. Because apoptosis secondary to injury prevents inflammation, our findings describe a novel mechanism on how PLTs contribute to tissue homeostasis. (*Blood*. 2015;126(12):1483-1493)

Introduction

At sites of tissue injury and endothelial damage, platelet (PLT) recruitment and accumulation are early key steps triggering a complex response to restore tissue integrity.[1-4] Upon attachment to an endothelial wound, PLTs become activated, spread out over the lesion, and recruit other PLTs, forming a wound sealing thrombus.[1,5] Recently, various effects on tissue remodeling have been attributed to PLTs including modulation of regeneration, inflammation, and tissue homeostasis.[6-8] PLT dysregulation contributes significantly to initiation or progression of pathologies.[5,9,10] Accordingly, the pathogenetic role of PLTs has been demonstrated in diseases of high socio-economic relevance including atherosclerosis or ischemic stroke,[11,12] but also in unexpected disease settings such as multiple sclerosis[13] or rheumatoid arthritis.[14] In the latter, PLTs amplify inflammation via collagen-dependent microparticle production,[14] whereas in the former, PLT activation contributes to neuronal tissue damage by recruitment and activation of inflammatory cells.[13] Besides these mechanisms, PLTs may balance tissue homeostasis in various previously unappreciated ways. Given the spatiotemporal relationship between PLT activation and initiation of apoptosis in injured tissues, PLTs may induce apoptosis following disruption of tissue integrity.

In multicellular organisms, damaged or superfluous cells are removed by programmed cell suicide.[15,16] The apoptosis program controls cell turnover, regulates the immune response, and eliminates defective cells, thereby balancing tissue homeostasis.[15,17,18] By eliminating damaged cells and their content, apoptosis generally avoids tissue inflammation with potential long-term defects in contrast to other forms of cell death.[17,19] Apoptosis can be induced via death receptor-mediated (extrinsic) or mitochondrial (intrinsic) signaling.[20,21] The intrinsic

Submitted December 15, 2013; accepted July 6, 2015. Prepublished online as *Blood* First Edition paper, July 31, 2015; DOI 10.1182/blood-2013-12-544445.

The online version of this article contains a data supplement.

The publication costs of this article were defrayed in part by page charge payment. Therefore, and solely to indicate this fact, this article is hereby marked "advertisement" in accordance with 18 USC section 1734.

pathway is activated in response to cellular stress such as DNA damage or growth factor deprivation. Cells are committed to apoptosis when the proapoptotic Bcl-2 proteins Bax and Bak permeabilize the outer mitochondrial membrane (OMM), leading to the cytosolic release of intermembrane proteins such as cytochrome c.[21,22] The activity of Bax and Bak is triggered by BH3-only proteins and inhibited by pro-survival Bcl-2 proteins in a complex network that involves the regulation of Bax shuttling on and off the OMM.[23,24]

The extrinsic apoptosis pathway depends on the activation of cell surface receptors such as the death receptor Fas (CD95, APO-1). Fas is a member of the tumor necrosis factor receptor family with an intracellular domain that forms trimers prior to activation.[25,26] Although Fas is widely expressed in human tissues, its ligand Fas ligand (FasL, CD95L) is primarily expressed by activated T cells, natural killer (NK) cells, and monocytes.[27] FasL occurs in a soluble and a membrane-bound form, but only the latter was shown to be involved in apoptosis induction.[28] Ligation of Fas triggers the activation of pro-caspase 8 and downstream caspase 3. In addition, the BH3-only protein Bid can be processed by caspase 8 to truncated Bid, which activates Bax and Bak on the OMM and, thus, initiate mitochondrial apoptosis signaling.[29,30] Although it is accepted that Fas signaling is important for apoptosis induced by tissue damage, the origin of the apoptosis signal following injury remains unclear. In this study, we describe a novel role of PLT membrane-bound FasL in apoptosis secondary to tissue injury.

Materials and methods

Mice

C57BL/6 mice were obtained from The Jackson Laboratory and bred in our animal facility. Mice lacking the membrane-bound part of FasL ($FasL^{\triangle m/\triangle m}$ mice) were generated and described recently.[28] Littermates were compared with each other and wild-type (WT) littermates served as control. Mice deficient for glycoprotein (GP) Ibα featuring severe thrombocytopenia[31] were kindly provided by Dr Jerry Ware (University of Arkansas). Animal experiments were approved by governmental authorities and performed in accordance with the German law guidelines of animal care. $FasL^{fl/fl}$ mice were described by Dr S. Karray (INSERM, France) before.[32] $FasL^{fl/fl}$ mice, which we kindly received from Dr Martin-Villalba (University of Heidelberg) were crossed to PF4-Cre mice, which we acquired from The Jackson Laboratory (C57BL/6-Tg [Pf4-cre] Q3Rsko/J). PF4-Cre^{+} $FasL^{fl/fl}$ mice or PF4^{-}Cre^{-} $FasL^{fl/fl}$ littermate controls were analyzed for tissue apoptosis using the transient middle cerebral artery occlusion (tMCAO) stroke model.

Isolation of PLTs and PLT membrane proteins

Human PLTs were isolated as described before.[33] Murine PLT preparations were obtained using a modified protocol.[34] Briefly, blood was drawn from the retro-orbital plexus via heparinized capillaries into a tube with 300 μL acid citrate-dextrose buffer (12.5 g sodium-citrate, 2 g citric acid, 10 g glucose in 500 mL distilled water, pH 4.7). To prevent PLT activation, apyrase and prostacyclin were used. To activate PLTs, isolated PLTs were stimulated at room temperature with 20 μM adenosine diphosphate (ADP), 25 μM thrombin receptor activating peptide (TRAP), or 0.2 U/mL thrombin. PLT activation was terminated by adding an equal volume of 4% paraformaldehyde (PFA) in phosphate buffered saline (PBS) to exclude any PLT-derived activity potentially affecting assay readouts. After incubation at 4°C for 30 minutes, fixed PLTs were washed thrice with PBS to remove any remaining PFA or activators, and resuspended in PBS. As positive control, 1 μM staurosporine (STS) was used. To isolate membranes from PLTs, the Mem-PER Eukaryotic Membrane Protein Extraction Reagent Kit (Thermo Scientific, Rockford, IL) was used. Isolated murine or human PLTs, extracted membranes, or soluble proteins from PLTs were used in subsequent experiments to induce apoptosis. PLT activation was monitored by flow cytometry using an anti-mouse P-selectin (CD62P) antibody (Ab) (Wug.E9; Emfret Analytics, Eibelstadt, Germany). To assure clean PLT preparations, we quantified leukocyte contamination using the Leucocount Kit (BD Biosciences, Heidelberg, Germany) as described by Burkhart et al.[35]

Isolation of primary murine neuronal cells and bone marrow-derived macrophages

Neuronal cell cultures were obtained from WT C57BL/6 mouse embryos (embryonic day 18) following previous protocols.[36] Briefly, pregnant mice were euthanized by cervical dislocation, and embryos were removed and transferred into warmed Hank's Balanced Salt Solution (HBSS) (Invitrogen, Darmstadt, Germany). After preparation of hippocampi, tissue was collected in 5 mL of 0.25% trypsin in HBSS. After 5 minutes of incubation at 37°C, the tissue was washed twice with HBSS and dissociated in 1 mL of neuronal medium (10% 10× Modified Earl's medium, 0.22% sodium bicarbonate, 1 mM sodium pyruvate, 2 mM L-glutamine, 2% B27 supplement [all from Invitrogen], 3.8 mM glucose [Merck, Darmstadt, Germany], and 1% penicillin/streptomycin [Biochrom, Berlin, Germany]) by triturating with fire-polished Pasteur pipettes of decreasing tip diameter. Neurons were diluted in neuronal medium and plated at a density of 60 000 cells/cm^2 on poly-*d*-lysine-coated (Sigma, Steinheim, Germany) coverslips in 4-well plates. All cell cultures were incubated at 37°C and 5% CO_2 for up to 5 to 7 days before experiments.

Hippocampal cell cultures were incubated with PLT lysates at the indicated dilutions for 24 hours. To analyze cell death, cultures were stained with 0.5 μg/mL 4,6 diamidino-2-phenylindole (DAPI) (Merck) or primary Abs against NEUronal Nuclei (NeuN) (1:1000; Millipore, Darmstadt, Germany) and active caspase 3 (1:800; Cell Signaling Technology, Frankfurt, Germany). Secondary cyanine 2-labeled donkey anti-mouse and Cy3-labeled goat anti-rat Abs were obtained from Dianova (Hamburg, Germany) and used at a 1:100 dilution. Negative controls were obtained by omitting the primary or secondary Ab and revealed no detectable signal (not shown). For quantification, samples were analyzed in a blinded fashion using fluorescence microscopy.

Bone marrow-derived macrophages were isolated as described previously.[37] The medium was changed every second day, loosely adherent dendritic cells were removed after 1 week, and the adherent macrophages were collected and used for experiments.

Flow cytometry

Flow cytometry was generally performed as described.[38,39] Briefly, fixed blood cells or isolated PLTs (as indicated in figure legends) were resuspended, diluted 1:25 with fluorescence-activated cell sorter (FACS) buffer (0.5% bovine serum albumin; 0.1% sodium azide in PBS), and stained with anti-mouse FasL-Biotin (MFL-3) Ab, anti-human FasL-PE (NOK-1) Ab, or with the corresponding immunoglobulin (Ig)G control (P36281; all from eBioscience, San Diego, CA) for 30 minutes at room temperature in the dark. Afterward, the samples were washed with FACS buffer and murine samples were stained with Streptavidin Alexa Fluor 488 (Invitrogen) for 30 minutes at room temperature in the dark. To compare levels of PLT FasL with those of leukocytes, macrophages were stained using an anti-CD11b PerCP and an anti-CD178 PE (MFL-3) Ab, or with the corresponding IgG control Ab (all from BioLegend) for 30 minutes at room temperature in the dark. Finally, samples were washed with FACS buffer and analyzed with a FACS Calibur flow cytometer (Becton Dickinson, Heidelberg, Germany). For detection of PLT contact with apoptotic cells, the right cerebral hemisphere with the insult and the unaffected contralateral hemisphere (control) were processed separately through a 40-μm cell strainer. Cell suspensions were stained in PBS supplemented with 2% fetal bovine serum and 0.5% bovine serum albumin with specific Abs for anti-CD45.2 eF450 (clone 104) and anti–CD41-APC (clone eBioMWReg30; both eBioscience, San Diego, CA), as well as with Annexin V fluorescein isothiocyanate (FITC) and propidium iodide (PI) according to the manufacturer's instructions using an Annexin V-FITC Apoptosis Detection Kit (BD Biosciences). Single PLTs were gated out via forward scatter and side scatter. Data were acquired on a FACSCanto II (BD Biosciences) and analyzed with FloJo (Tree Star, Ashland, OR).

Western blotting

For whole cell lysates, mouse embryonic fibroblasts (MEFs)[40] and PLTs were harvested and subjected to acetone precipitation, resuspended in sodium dodecyl sulfate sample buffer, and boiled for 10 minutes at 95°C. Finally, samples were separated by sodium dodecyl sulfate-polyacrylamide gel electrophoresis and subjected to western blot as described before.[13] Afterward, membranes were blocked with 5% skim milk in Tris-buffered saline 0.05% Tween-20 and incubated with primary Abs at 4°C overnight. Secondary Ab was incubated 1 hour at room temperature and membranes were washed thrice with Tris-buffered saline 0.05% Tween-20. Finally FasL, tumor necrosis factor-related apoptosis-inducing ligand (TRAIL) and Tom20 as loading control were detected using anti-mouse FasL (Cell Signaling), anti-TRAIL (Abcam, Cambridge, United Kingdom), and anti-Tom20 Ab (Santa Cruz Biotechnology, Dallas, TX).

Confocal microscopy

Resting fixed PLTs were immobilized on poly-L-lysine–coated coverslips and co-stained using an anti-CD62P (Abcam) and an anti-FasL Ab (Abcam). To analyze the presence of PLTs after induction of stroke in the brain tissue in vivo, we co-stained murine brain sections with Abs using the endothelial marker CD31 (Abcam), the neuronal marker NeuN (Millipore), and the PLT marker GPIbα (POP/B; Emfret Analytics). Primary Abs were incubated at 4°C overnight and fluorescent secondary Abs (Dianova) for 1 hour at room temperature. Nuclei were stained using DAPI (displayed in white in Figure 1A using Leica Confocal Software version 2.61). Primary Abs were detected using secondary Ab anti-rat 549 (PLTs, red), anti-rabbit 488 (endothelium, green), and anti-mouse Cy5 (neurons, blue). Samples were analyzed by standard confocal immunofluorescence microscopy (Leica TCS SP2, DM IRE2).

Detection of apoptosis

For the different cell types, the time point for detection of apoptosis varied. SH-SY5Y neuroblastoma cells were co-incubated with PLTs for 6 hours. To detect apoptosis via measurement of caspase 3/7 activity, activated PLTs were immobilized onto a 96-well plate, fixed with PFA, washed thrice with PBS, and incubated with cells at 37°C. Afterward, cells were incubated with Apo-ONE caspase 3/7 reagent (Promega, Mannheim, Germany) according to the manufacturer's recommendations. Repeats are provided as n = wells analyzed. For TdT-mediated dUTP-biotin nick end labeling (TUNEL) staining, the in situ Cell Death Detection Kit, TMR red was used according to the manufacturer's instructions (Roche, Filderstadt, Germany). Cells were seeded onto chamber slides. The next day, activated fixed PLTs or saline were added and co-incubated for 16 hours. For quantification, 8 different microscopic fields per section were counted and the percentage of TUNEL-positive cells was determined. For transwell assays, a Boyden chamber (polycarbonate membrane filter pores 5 μm, Neuro Probe; Gaithersburg, MD) was used. Resting or ADP-activated PLTs (2×10^8) were added to the lower chamber, SH-SY5Y (2×10^4) to the upper chamber, or both SH-SY5Y (2×10^4) cells and activated PLTs were added to the lower chamber. After 16 hours of incubation, Annexin V staining was performed using the FITC Annexin V Apoptosis Detection Kit I from BD Pharmingen (Heidelberg, Germany).

Induction of apoptosis using the PLT membrane fraction

For caspase 3/7 measurements, SH-SY5Y cells or MEFs were seeded in 96-well plates and treated with serial dilutions of protein fractions extracted from human PLTs, or from murine WT or FasL$^{\triangle m/\triangle m}$ PLTs. After 6 hours incubation, Apo-ONE caspase 3/7 reagent (Promega) was applied, and the fluorescence signal was measured in 1 minute intervals with an excitation wavelength of 490 nm and an emission wavelength of 520 nm in a plate reader. Repeats are provided as n = wells analyzed. Due to hydrophobic buffer effects, apoptosis activity was normalized to the corresponding samples from mock-stimulated PLTs.

Measurement of lactate dehydrogenase (LDH) release

For measurements of LDH release, SH-SY5Y cells or MEFs were seeded in 96-well plates and treated with serial dilutions of protein fractions obtained from human PLTs or from murine WT or FasL$^{\triangle m/\triangle m}$ PLTs. After 6 hours incubation, CytoTox 96 reagent (Promega) was applied and the absorbance at 490 nm was measured in a plate reader. Total levels of cellular LDH were determined by lysis of untreated cells. Repeats are provided as n = wells analyzed. In some experiments, MEFs deficient for Bax and Bak (double knockout [DKO]) cells[40] were applied to evaluate the relevance of the intrinsic pathway to PLT-induced apoptosis.

N-methyl-D-aspartic acid (NMDA) retina injury model

For the NMDA model, all experiments were approved by the Animal Care and Use Committee at the National Eye Institute, National Institutes of Health (animal study protocols 06-553, 06-570, and 07-608), and were performed according to the National Institutes of Health guidelines and regulations on animal studies. The NMDA retinal injury model was performed and results were analyzed as described previously.[41] For PLT depletion, PLT-depleting serum (10 μL in PBS, intraperitoneal [IP]; Accurate Chemical and Scientific, Westbury, NY) or control serum was applied 24 hours before induction of apoptosis by NMDA injection. To monitor PLT depletion, whole blood was taken from mice treated with control serum or PLT-depleting serum (10 μL in PBS, IP) and the number of PLTs was analyzed with an automated cell counter (Sysmex).

Stroke model

All stroke experiments were performed in accordance with the recently published ARRIVE guidelines (NC3Rs). Animals were randomly assigned to the treatment groups. For PLT depletion, PLT-depleting serum (10 μL in PBS, IP) or control serum was applied 24 hours before tMCAO.[42] For depletion of macrophages, clodronate liposomes or control liposomes were injected into mice as described before.[37] Furthermore, in some experiments, GPIIb-IIIa was inhibited to prevent intravascular thrombosis by injection of 100 μg anti–GPIIb-IIIa F(ab)$_2$ or control IgG as described before.[43] Focal cerebral ischemia was induced by tMCAO using the intraluminal filament technique as described.[43,44] Animals were anesthetized with 2.5% isoflurane in a 70% N_2O/30% O_2 mixture and body temperature was maintained at 37°C throughout surgery. Following a midline skin incision in the neck, the proximal common carotid artery and the external carotid artery were ligated, and a standardized silicon rubber-coated 6.0 nylon monofilament (6021; Doccol, Sharon, MA) was inserted and advanced via the right internal carotid artery to occlude the origin of the middle cerebral artery. After 60 minutes, the filament was withdrawn to allow reperfusion. Mice were euthanized 24 hours after MCAO. Brains were quickly removed and embedded for cryosections.[45] To analyze apoptosis, the in situ Cell Death Detection Kit, TMR red was used according to the manufacturer's instructions.

Data presentation and statistics

Comparisons between group means were performed using Student *t* test or one-way analysis of variance. $P < .05$ was considered statistically significant. Error bars indicate standard error of the mean (SEM).

Results

PLT depletion reduces tissue apoptosis in vivo

Vascular and tissue injury result in thrombus formation and subsequent tissue remodeling featuring apoptosis to remove damaged cells. Whether PLTs influence processes contributing to tissue damage and remodeling beyond thrombus formation is currently not known. Following stroke, we detected PLTs outside the vasculature in ischemic mouse brains (Figure 1A-B). Furthermore, using a flow cytometry based approach, we observed an increase in CD41-positive PLTs associated with CD45-negative Annexin V-positive cells upon induction of stroke. This increase was ~60% for early apoptosis (Annexin V-positive/PI-negative cells) and ~50% for late apoptosis (Annexin V-positive/PI-positive cells)

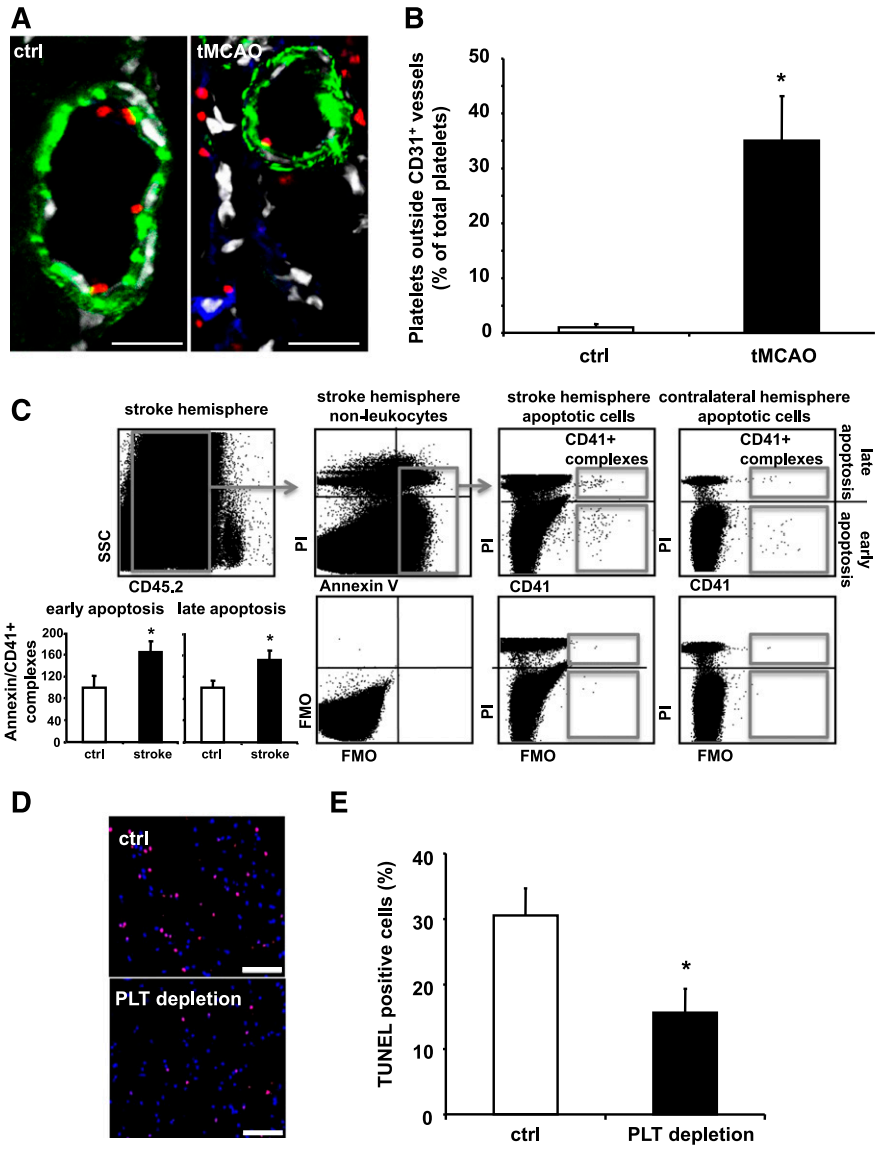

Figure 1. PLT depletion reduces apoptosis in a murine stroke model in vivo. (A-E) Stroke was induced in C57BL/6 mice by tMCAO for 60 minutes. (A-B) Ischemic brain tissues were co-stained for PLT GPIbα (red), neuronal cells (NeuN, blue), and endothelial cells (CD31, green). Nuclei were stained using DAPI (displayed in white using Leica Confocal software version 2.61). Scale bar, 20 μm. (A) Shows representative images. (B) For quantification, PLTs outside of vessels were counted in a blinded fashion using fluorescence microscopy in healthy and ischemic brain tissue. Data are mean ± SEM and show the percentage of total PLTs per section (n = 6, 3 non-consecutive sections per animal were analyzed). (C) Identification of early (Annexin V^+, PI^-) and late (Annexin V^+, PI^+) apoptosis in $CD45.2^-$ nonleukocytes that complex with $CD41^+$ PLTs in stroke tissue and the contralateral control hemisphere (upper panel). Percentage of $CD41^+$ PLT complexes with apoptotic nonleukocytes in the stroke hemisphere relative to the corresponding contralateral hemisphere was calculated (n = 4). Results are presented as mean ± SEM, $*P < .05$ (left, lower panel). FMO staining controls document staining specificity and gating strategy (right, lower panel). (D-E) Prior to stroke induction, animals were treated with either control serum (ctrl) or PLT-depleting serum (PLT depletion) resulting in more than 90% of PLT depletion (supplemental Figure 1). (D) Shows representative images of stained tissue sections from a control serum or PLT-depleting serum-treated mouse after induction of stroke. Nuclei were stained with DAPI (blue) and TUNEL-positive cells are depicted in red. Scale bar, 100 μM. (E) Quantification of apoptotic cells upon injection of control serum or PLT-depleting serum. For quantification, apoptotic cells were counted in a blinded fashion using fluorescence microscopy. Data are mean ± SEM and show the percentage of TUNEL-positive cells of total cell number per section (n = 6). $*P < .05$ vs control treated animals. FMO, fluorescence minus one.

(Figure 1C) in comparison with the contralateral control hemisphere. These findings prompted us to assess tissue apoptosis in the presence or absence of PLTs. C57BL/6 mice were treated with PLT-depleting serum (ie, PLT depletion) or control serum (ctrl), before they underwent tMCAO for 60 minutes. PLTs were efficiently depleted following anti-PLT serum application (see supplemental Figure 1 on the *Blood* Web site). After tMCAO, ~30% of TUNEL-positive apoptotic cells were detected in mock-treated animals (Figure 1D-E). In PLT-depleted animals, however, the number of TUNEL-positive cells after tMCAO-induced cell damage decreased to approximately half of the apoptotic cell pool in mock-treated animals (Figure 1D-E). Similarly, in GPIbα-deficient mice featuring severe thrombocytopenia, tissue apoptosis was significantly reduced compared with WT mice (supplemental Figure 2).

It is well accepted that PLTs may aggravate tissue damage by reenforcement of inflammatory processes.[5] To further dissect the role of PLTs for apoptosis in vivo in a setting of negligible levels of tissue inflammation, we applied an NMDA-induced model of retinal apoptosis.[41] For this purpose, NMDA was injected into the vitreous cavity of C57BL/6 mice. When mice had been pretreated with PLT-depleting serum, retinal apoptosis was reduced by ~40% (Figure 2A-B), showing that PLTs contribute to programmed cell death also in a setting of low-tissue inflammation. Interestingly, we observed no difference in tissue apoptosis after induction of stroke, when animals were pretreated with a blocking F(ab) against GPIIb-IIIa, which abolishes intravascular thrombosis (Figure 2C). Thus, receptors other than GPIIb-IIIa seem to mediate PLT-induced apoptosis in the neuronal tissue in vivo.

PLTs induce apoptosis in human and mouse neuronal cells

The direct effect of PLTs on human cells was tested by incubation of ADP-activated PLTs with cultured SH-SY5Y neuroblastoma cells. Significant leukocyte contamination of PLT isolations (<1 leukocyte per 10^6 PLTs) was excluded (data not shown). Analysis of caspase 3/7 activity showed that PLTs induce apoptosis in neuroblastoma cells in a concentration-dependent manner (Figure 3A), whereas ADP itself had no effect (data not shown). PLT activation was confirmed by expression of the activation marker P-selectin (supplemental Figure 3). PLT-induced caspase 3/7 activity was comparable to that of apoptosis stimulation by STS. Similarly, the presence of ADP-activated PLTs resulted in a significant increase in

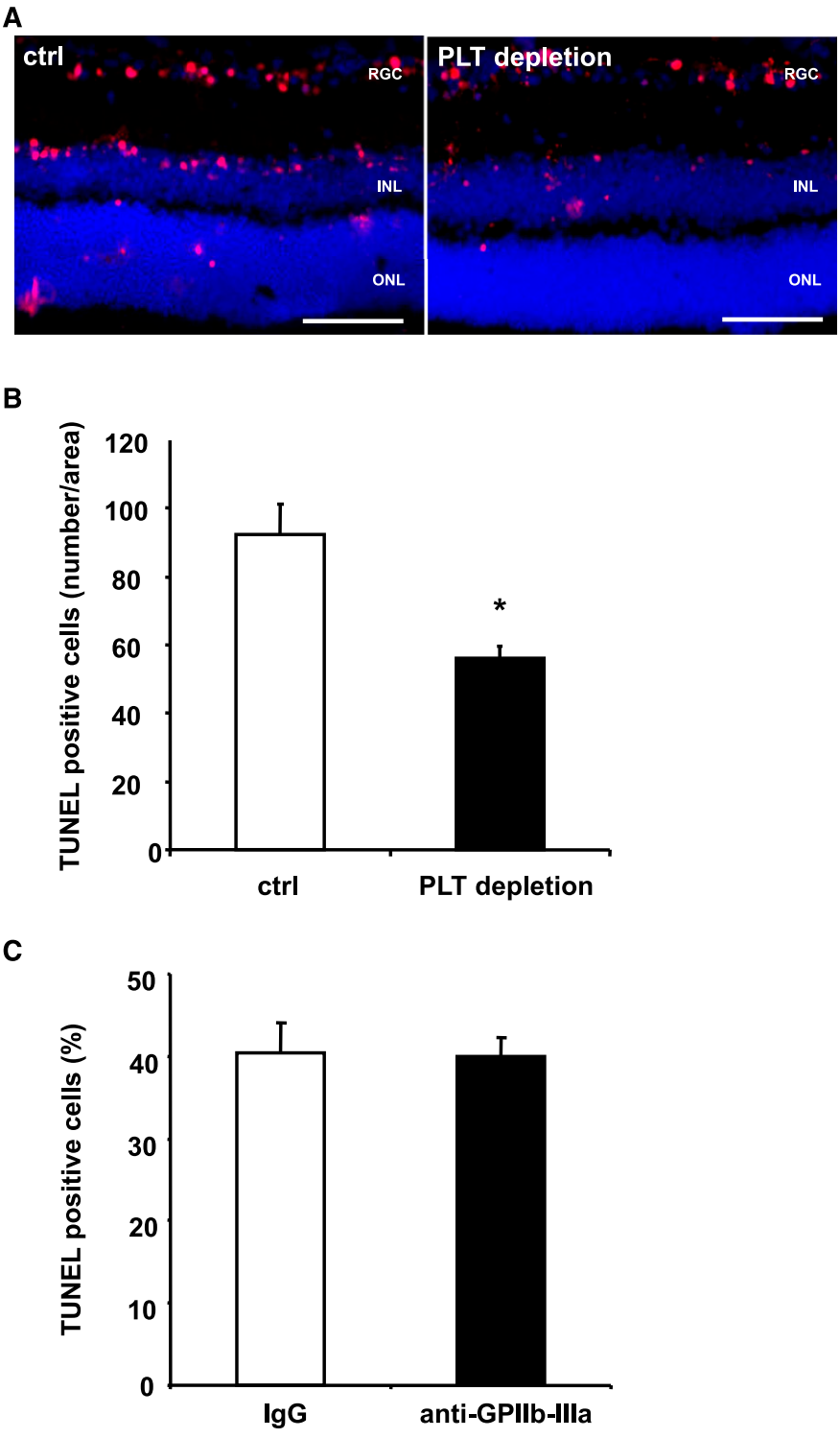

Figure 2. PLT depletion reduces apoptosis in a retinal model with low levels of inflammation, whereas inhibition of GPIIb-IIIa does not affect tissue apoptosis. (A-B) Mice were treated with control serum (ctrl) or PLT-depleting serum (PLT depletion). Subsequently, neuronal apoptosis was induced by intravitreal injection of NMDA. In this model of tissue apoptosis, levels of tissue inflammation are negligible. In retinal sections, TUNEL staining was performed and sections were analyzed in a blinded fashion using immunofluorescence microscopy. Eight non-consecutive sections were analyzed per animal. (A) Shows representative images. (B) Data are mean ± SEM and show the number of TUNEL-positive cells per area (n = 8). *$P < .05$ vs control treated animals. Scale bar, 100 μm. (C) Stroke was induced in C57BL/6 mice by tMCAO for 60 minutes. Animals were treated with a blocking anti–GPIIb-IIIa F(ab) 1 hour prior to stroke induction. Data are mean ± SEM and show the percentage of TUNEL-positive cells of total cell number per section (n = 5, 3 non-consecutive sections per animal were counted in a blinded fashion). No significant difference was observed between groups. INL, inner nuclear layer; ONL, outer nuclear layer; RGC, retinal ganglion cell.

TUNEL-positive SH-SY5Y cells (supplemental Figure 4). In order to distinguish between intracellular and membrane-associated mechanisms of PLT-induced apoptosis, SH-SY5Y cells were incubated with the membrane proteins or the soluble protein fraction of ADP-stimulated or unstimulated human PLTs. Induction of cell death was measured by LDH release.[46] The membrane protein fraction of ADP-stimulated PLTs robustly induced neuroblastoma cell death in a dose-dependent manner (Figure 3B). In contrast, low LDH activity was measured after treatment with the soluble protein fraction or the membrane proteins of unstimulated PLTs (Figure 3B). PLT-induced cell death correlated with an increase of caspase 3/7 activity in SH-SY5Y cells treated with membrane proteins of ADP-stimulated PLTs (Figure 3C). PLTs were also activated by thrombin or TRAP. Similar to ADP, both TRAP and thrombin-treated PLTs induced apoptosis in neuroblastoma cells (supplemental Figure 5). In addition, Boyden chamber experiments showed only apoptosis induction when PLTs and neuroblastoma cells were incubated in the same compartment (supplemental Figure 6). In

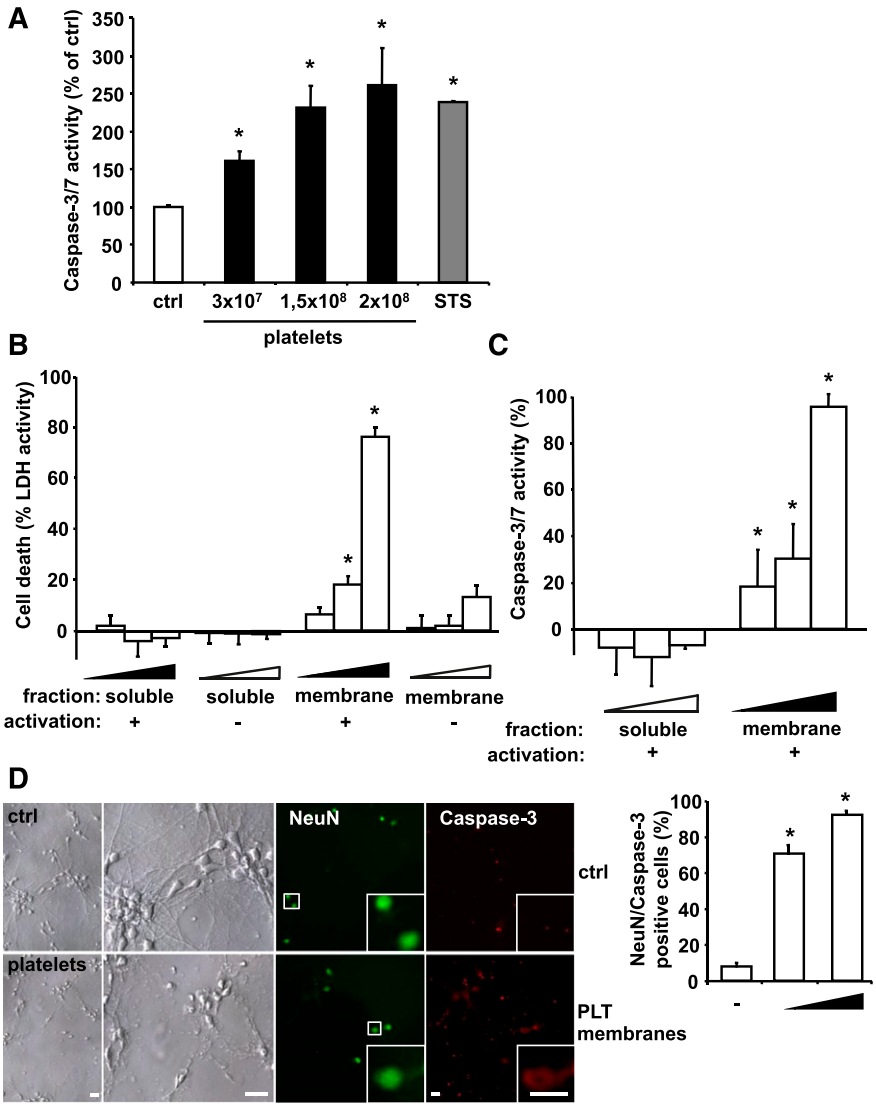

Figure 3. PLTs induce apoptosis in a dose-dependent manner in in vitro grown neuroblastoma cells. (A) Isolated human PLTs were stimulated with ADP, fixed with PFA to exclude PLT-derived signal, and incubated with SH-SY5Y neuroblastoma target cells. As positive control, cells were treated with 1 μM STS. After 6 hours, caspase activity was measured and calculated as mean ± SEM (n = 6). *$P < .05$ vs control. Results are expressed as percentage of buffer-treated control. (B) LDH activity was measured in the supernatant of cultured SH-SY5Y cells after application of various dilutions (4×10^{-4}; 4.5×10^{-4}; 5×10^{-4}) of isolated membrane protein and soluble fractions of buffer- (−) or ADP-stimulated (+) human PLTs for 6 hours. Data were normalized to the total LDH level from the same amount of untreated and lysed cells. Data represent mean ± SEM (n = 9) and are shown as percentage of total cellular LDH levels of untreated cells. *$P < .05$ vs corresponding soluble fraction or membrane fractions of resting PLTs. (C) Caspase 3/7 activity kinetics were measured in SH-SY5Y cells incubated with various dilutions (4×10^{-4}; 4.5×10^{-4}; 5×10^{-4}) of the isolated membrane protein and soluble fractions of ADP-stimulated human PLTs for 6 hours. Data were normalized to the corresponding samples from buffer-stimulated PLTs (control). Data represent mean ± SEM (n = 12) and are shown as percentage of control. *$P < .05$ vs corresponding soluble fraction. (D) Primary murine neuronal cells were incubated with buffer (ctrl) or with membrane proteins of ADP-activated murine PLTs (0.5×10^8 or 2.5×10^8 PLTs). To analyze cell death, cultures were co-stained for NeuN and active caspase 3. For quantification, staining was analyzed in a blinded fashion by fluorescence microscopy. Data are mean ± SEM (n = 5) and are shown as percentage of total cell number per section. *$P < .05$ vs control. Scale bar, 20 μm.

time course experiments, PLTs induced apoptosis signaling in neuroblastoma cells within 6 hours (supplemental Figure 7). To assess PLT-induced apoptosis in primary murine cells, apoptosis of neuronal cells isolated from the hippocampus of mouse embryos (embryonic day 18) was assessed after exposure to membrane proteins of ADP-activated murine PLTs. Similar to the experiments using cell lines, PLTs also induced increased caspase 3 activity in primary neuronal cells (Figure 3D).

Activated PLTs present membrane-bound FasL

The stimulation of cell death by PLTs in vitro suggests specific induction of apoptosis upon cell contact with activated PLTs. Interestingly, a minor pool of activated PLTs has previously been implicated in Fas-mediated tumor cell apoptosis.[47] Thus, the presence of death receptor ligands on PLTs was analyzed by western blot. We detected FasL protein but not the death receptor ligand TRAIL in murine PLTs irrespective of prior activation (Figure 4A). In contrast to Fas, which has a broader tissue distribution, the expression of FasL is mainly restricted to subsets of activated T cells, NKT cells, and NK cells.[27,48] Resting human PLTs presented low amounts of FasL on their surface, whereas activation of PLTs by ADP resulted in significant upregulation of FasL on their surface (Figure 4B). In parallel, upregulation of FasL surface expression upon ADP activation was also observed in murine PLTs (Figure 4C). Supplemental Figure 8 shows the relative expression level of surface FasL on murine ADP-activated PLTs in comparison with murine CD11b-positive macrophages. Confocal imaging suggested that FasL is stored in granula and partially co-localizes with CD62P (Figure 4D).

PLT-induced apoptosis is mediated by membrane-bound FasL

To further evaluate the effect of PLT FasL, we used mice deficient for membrane-bound but not soluble FasL ($FasL^{\triangle m/\triangle m}$ mice).[28] PLTs from these and WT animals were analyzed for their effect on apoptosis induction in MEFs. Interestingly, membrane fractions of ADP-stimulated PLTs from WT mice robustly induced dose-dependent cell death, whereas soluble fractions or membrane proteins from resting PLTs failed to induce cell death (Figure 5A). In contrast, membrane proteins of ADP-stimulated PLTs from $FasL^{\triangle m/\triangle m}$ mice did not induce apoptosis in MEFs, as analyzed by LDH release and caspase 3/7 activity (Figure 5A-B). Additionally, PLT membrane protein-induced apoptosis was inhibited with a blocking anti-FasL Ab in vitro (supplemental Figure 9). These results show that FasL exposed on membranes of ADP-stimulated PLTs induces apoptosis.

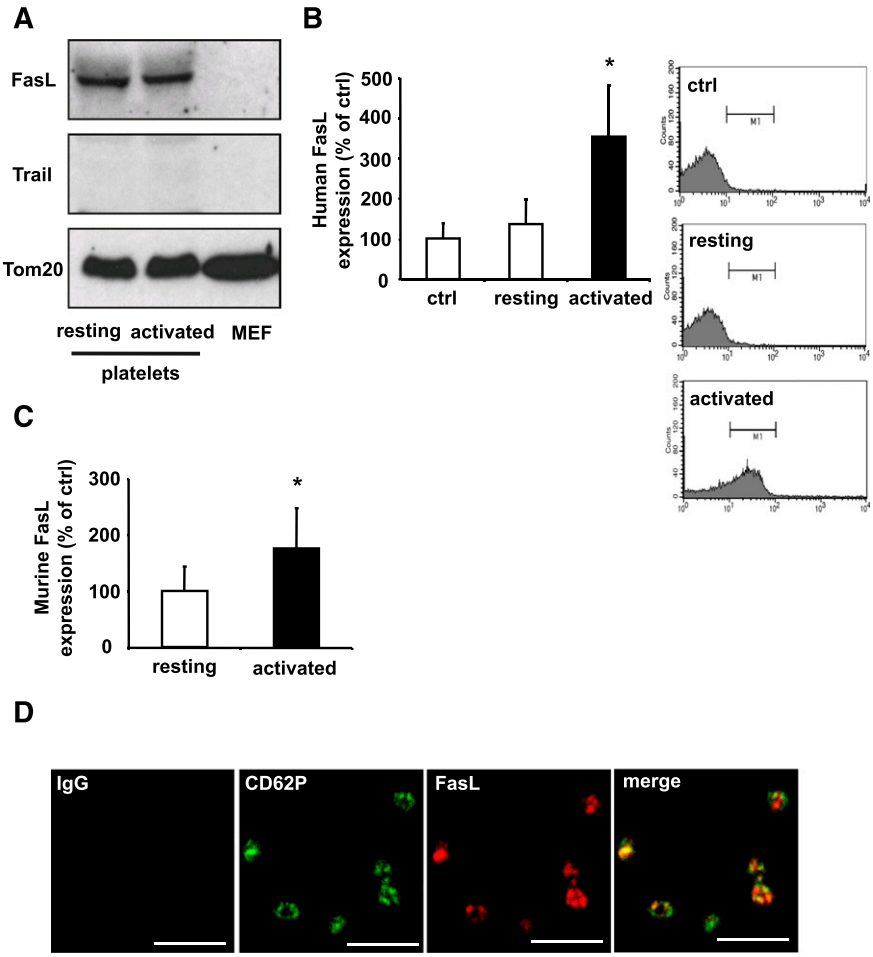

Figure 4. PLTs express FasL. (A) Expression levels of death ligands FasL and TRAIL in resting or ADP-activated murine PLTs and MEFs analyzed by western blot. Loading equivalency was assessed by Tom20 staining. (B) Human whole blood was stimulated with ADP (activated) or buffer (resting), fixed with PFA, and analyzed by flow cytometry. PLTs were gated by forward and side light scatter characteristics and analyzed for FasL expression using a PE-coupled FasL Ab. Data are mean ± SEM and are shown as percentage of control and IgG control represents the 100% control (n = 5). *$P < .05$ vs control. (C) Murine PLTs were stimulated with ADP and analyzed for surface expression of FasL by flow cytometry. Data are mean ± SEM and are shown as percentage of control. Resting PLTs represent the 100% control (n = 7). *$P < .05$ vs control. (D) PLTs were co-stained for the α-granular marker CD62P (green) and FasL (red). Staining was analyzed by confocal fluorescence microscopy. Scale bar, 5 μM.

The effect of mitochondrial Bax/Bak-dependent[49] apoptosis on PLT-induced cell death was analyzed by the application of soluble protein, or the membrane protein fractions of activated or resting WT or FasL$^{\triangle m/\triangle m}$ PLTs to Bax/Bak DKO MEFs. LDH activity measurements revealed a robust and concentration-dependent induction of cell death by membrane protein fractions isolated from activated PLTs of WT but not FasL$^{\triangle m/\triangle m}$ mice (Figure 5C). Subsequently, we visualized mitochondrial apoptosis signaling in SH-SY5Y cells expressing green fluorescent protein (GFP)-Bax after exposure to PLTs using confocal microscopy. Bax translocation to mitochondrial foci occurred in target cells after exposure to ADP-stimulated PLTs but not resting PLTs (Figure 5D). Bax translocation and activation, as revealed by staining with the conformation-specific Bax Ab 6A7, are two hallmarks of Bax activation and mitochondrial apoptosis. These results suggest that PLT-induced apoptosis does not require mitochondrial signaling, but can induce Bax activation and, thus, increase apoptotic cell death.

To further characterize the role of PLT surface-exposed FasL in vivo, we induced stroke in PF4-Cre^{+} FasL$^{fl/fl}$ mice. These mice deficient for FasL in the megakaryocytic lineage have similar PLT counts (Figure 6A) and similar ADP-induced aggregation (data not shown) compared with their Cre^{-} littermate controls. Furthermore, expression of important receptors for PLT function (supplemental Figure 10) and bleeding time (Figure 6B) were not different between WT and FasL PLT-deficient mice, respectively. Interestingly, however, we found that apoptosis in PF4Cre^{+} FasL$^{fl/fl}$ animals was reduced in comparison with PF4Cre^{-} FasL$^{fl/fl}$ mice (Figure 6C-D). This difference persisted after depletion of macrophages using clodronate liposomes (Figure 6E).

Discussion

PLTs play a central role in the pathogenesis of cardiovascular and inflammatory diseases.[5,50] Their activation can occur in close spatiotemporal proximity to programmed cell death of damaged cells at sites of tissue disruption. Our results show that activated PLTs induce apoptosis in human and murine cells. FasL exposed on the cell membrane upon PLT activation induced target cell apoptosis within 6 hours. The requirement of the membrane-bound form of FasL has been previously established for T cells.[28] Membrane-bound FasL has been shown to trigger aggregation of pre-assembled Fas trimers on the target plasma membrane and, thus, the initiation of caspase 8-dependent death receptor-mediated apoptosis in the target cell.[51-53] Caspase 8-dependent activation of the BH3-only protein Bid induced mitochondrial apoptosis signaling and, thus, increased the cell death response to death receptor activation.[29,30] Consequently, PLT-induced apoptosis in human neuroblastoma cells was followed by Bax translocation, and the apoptotic response of MEFs was reduced in the absence of Bax and Bak.

A substantial reduction of tissue apoptosis after PLT depletion could be observed in both tMCAO-induced cell death and NMDA-induced retinal apoptosis. These findings establish a contribution of PLTs to tissue apoptosis in vivo. Interestingly, the inhibition of GPIIb-IIIa does not alter apoptosis within the stroke tissue. Thus, mechanisms other than the engagement of this integrin account for PLT-induced apoptosis. Here, we have identified PLT-derived FasL as one mechanism, but future studies will have to address the contribution of other potential mechanisms in PLT-induced apoptosis.

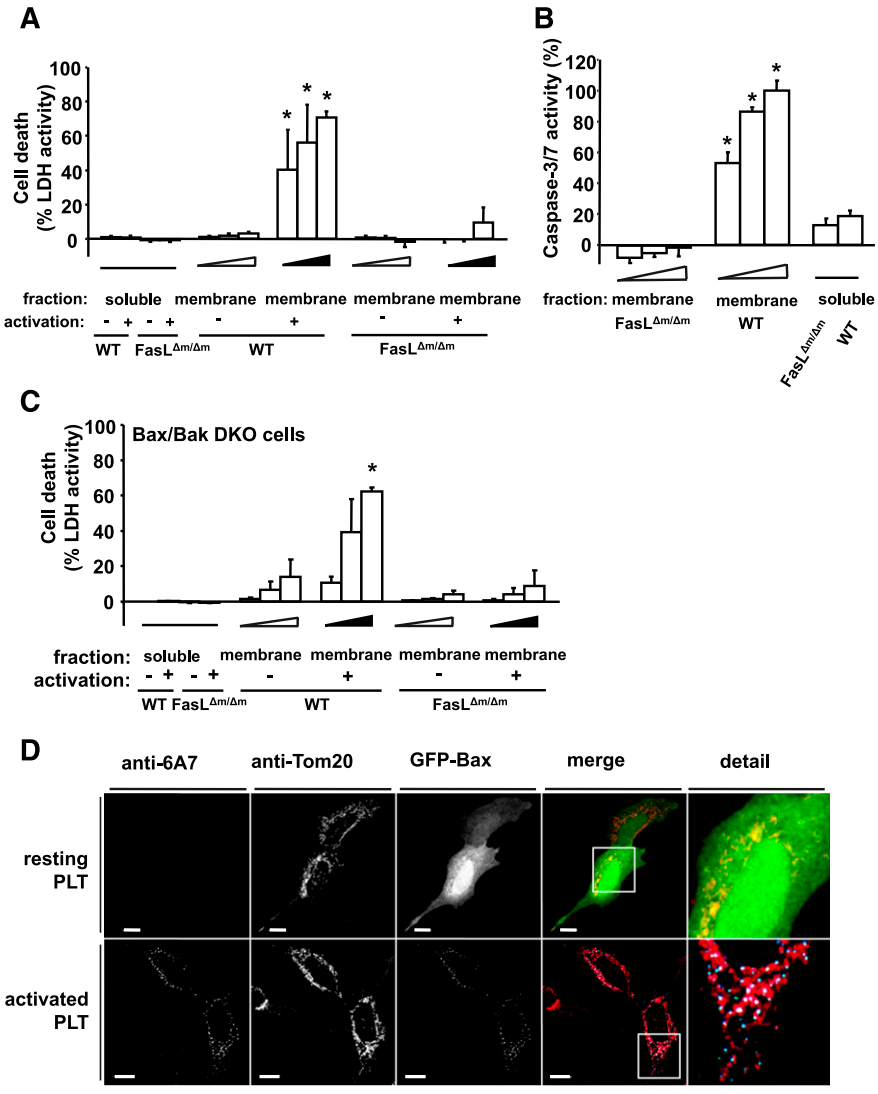

Figure 5. PLT membrane protein induces apoptosis via membrane-bound FasL. (A) MEFs were incubated with various dilutions (4×10^{-4}; 4.5×10^{-4}; 5×10^{-4}) of membrane proteins (membrane fraction) of buffer- or ADP-stimulated PLTs from WT mice or FasL$^{\Delta m/\Delta m}$ mice (lacking membrane-bound FasL only) for 6 hours. Isolated soluble proteins (soluble fraction) of buffer- or ADP-stimulated PLTs from WT mice or FasL$^{\Delta m/\Delta m}$ mice were incubated in a dilution of 5×10^{-4} of the protein sample. Subsequently, LDH activity was measured. Data represent mean ± SEM (n = 9) and are shown as percentage of total cellular LDH levels of untreated cells. *$P < .05$ vs FasL$^{\Delta m/\Delta m}$, soluble- and membrane-fraction of resting WT PLTs. (B) Caspase 3/7 activity kinetics were measured in MEFs incubated with various dilutions (4×10^{-4}; 4.5×10^{-4}; 5×10^{-4}) of the isolated membrane protein fraction of ADP-stimulated PLTs from WT or FasL$^{\Delta m/\Delta m}$ mice for 6 hours. Isolated soluble proteins (soluble fraction) were incubated in a dilution to 5×10^{-4} of the protein sample. Data were normalized to the corresponding samples from resting PLTs. Data are shown as percentage of control and represent mean ± SEM (n = 6). *$P < .05$ vs FasL$^{\Delta m/\Delta m}$ or soluble fractions. (C) LDH activity was measured after 6 hours in the supernatant of mitochondrial apoptosis-incompetent Bax/Bak DKO MEFs incubated with various dilutions (4×10^{-4}; 4.5×10^{-4}; 5×10^{-4}) of membrane protein (membrane fraction) of resting or ADP-stimulated PLTs from WT or FasL$^{\Delta m/\Delta m}$ mice. Soluble proteins (soluble fraction) were incubated in a dilution to 5×10^{-4} of the isolated proteins. Data represent mean ± SEM (n = 6) and are shown as percentage of total cellular LDH levels of untreated cells. *$P < .05$ vs FasL$^{\Delta m/\Delta m}$, soluble fraction or membrane fraction of resting WT PLTs. (D) SH-SY5Y cells transfected with GFP-Bax were incubated with resting or ADP-stimulated and PFA-fixed PLTs for 6 hours. Co-localization of GFP-Bax fluorescence (green) with mitochondrial Tom20 staining (red) is shown in yellow in the merged panel. Bax activation was detected with the conformation-specific anti-Bax Ab 6A7. Co-localization of active Bax and mitochondrial Bax is shown in cyan and white, respectively, in the merged panel. Bars, 10 μm.

PLT-dependent cell death appears diffuse in the applied models, possibly caused by target cells releasing soluble factors, eg, cytokines prior to or after commitment to apoptosis.[54,55] In addition to apoptosis induction, Fas signaling stimulates the production of cytokines and chemokines and, thus, the immune response toward dying cells.[54] PLT-mediated Fas signaling may therefore induce apoptosis and efficient removal of damaged cells to restore tissue integrity. In addition, a diffuse contact interface between PLTs and the tissue is conceivable, as during stroke, several pathomechanisms result in leakiness of the vasculature, particularly the microcirculation.[42,56]

Previously, FasL-dependent apoptosis has been found to prevent destructive inflammatory responses following viral infection in the eye.[57] Our results suggest that PLTs not only play an important role in the apoptotic response to cell damage in the retina but potentially also other tissues. They may also provide a rationale for the contribution of PLTs to the pathogenesis of multiple sclerosis.[13]

PLT activation is a prerequisite for FasL membrane exposure, preventing otherwise constitutive apoptosis induction and, thus, uncontrolled tissue damage. This notion is in accordance with the previous observation that PLTs can induce apoptosis of endothelial cells in vitro.[58,59] Consistent with our findings, the study observed the requirement of PLT activation, but did not identify the dependency on PLT-derived FasL for endothelial cell death. Interestingly, activated megakaryocytes were shown to express membrane-bound FasL, but the function remained unclear.[60]

Tissue or endothelial injury is a pathophysiological setting with PLT activation, where PLTs are the first cells to reach the wound and get activated.[1,9] Our results suggest a contribution of PLTs to tissue apoptosis besides their classical function to initiate the restoration of tissue integrity[7] and to promote long-range regenerative mechanisms.[7,61] In contrast to uncontrolled tissue damage, programmed cell death is an important mechanism to maintain tissue homeostasis.[15,17,18,62,63] In the context of sepsis, Clark et al[64] found that PLT interaction with neutrophils can mediate endothelial damage in the presence of lipopolysaccharide. Although cell damage was measured by PI uptake, endothelial apoptosis was not assessed.[64] In line with our findings, Ahmad et al[47] showed that human PLTs contain FasL upon activation and induce apoptosis in Fas-positive tumor cells. Although our results clearly point toward a role of PLTs for tissue apoptosis, their contribution could also involve further propagation via other cell types, including inflammatory cells. The previously unappreciated process of PLT-induced apoptosis may prevent uncontrolled cell death and, thus, negative tissue remodeling with potentially interesting clinical implications. Although stroke is a devastating disease, therapeutic options for treatment of ischemic stroke are very limited, and less than 5% of patients are

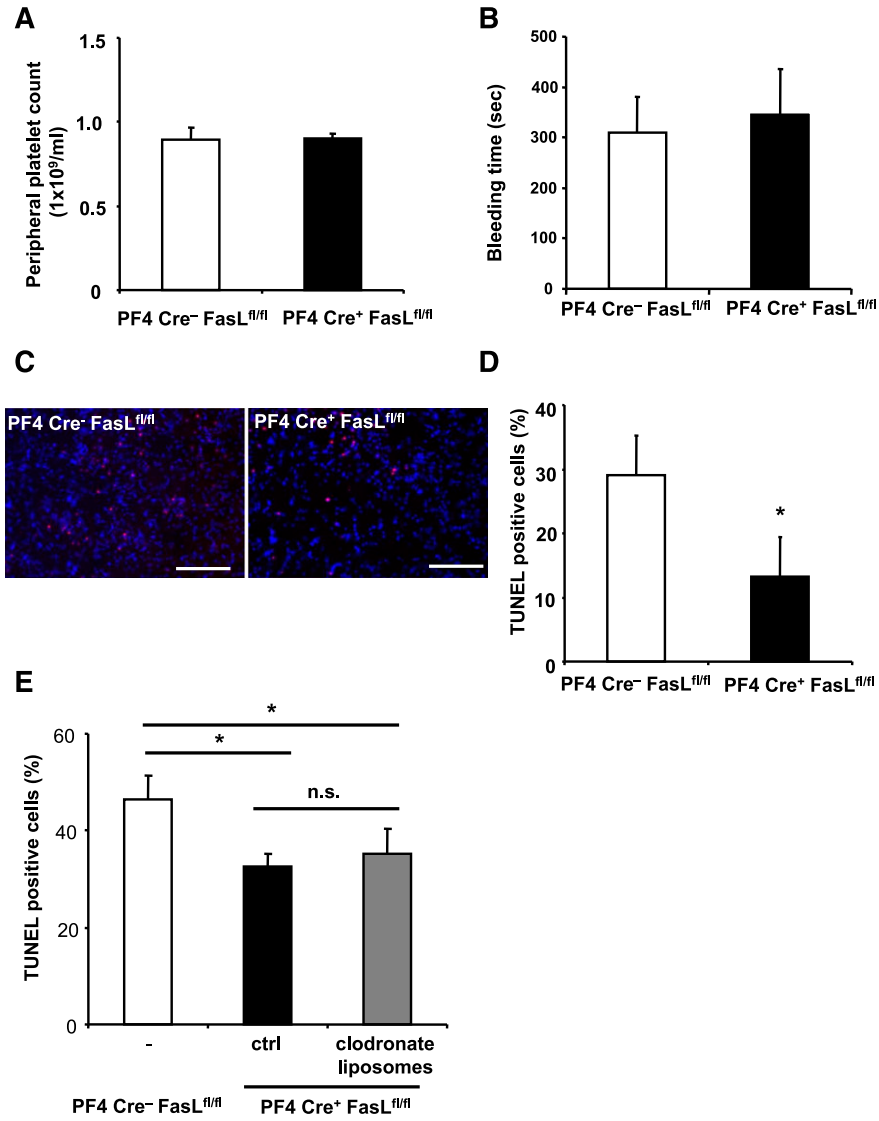

Figure 6. PLT-derived FasL contributes to tissue apoptosis in vivo. (A-E) PF4-Cre^{+} FasL$^{fl/fl}$ mice were generated and stroke was induced by tMCAO. PF4-Cre^{-} FasL$^{fl/fl}$ mice served as control. (A-B) We observed no difference in peripheral PLT counts and bleeding time between Cre^{-} littermates and PF4-Cre^{+} FasL$^{fl/fl}$ mice. (C-D) Apoptosis was quantified in brain sections using TUNEL staining. Neuronal apoptosis is presented as the percentage of TUNEL positive cells (red) of total cell number per section. Nuclei were stained using DAPI (blue). Data are mean ± SEM (n = 6, 5 non-consecutive sections per animal were analyzed). *$P < .05$ vs control animals. (C) Depicts representative images of the analyzed sections. (E) PF4-Cre^{+} FasL$^{fl/fl}$ mice were injected with control liposomes or clodronate liposomes to deplete macrophages before stroke induction, and apoptosis was assessed within the brain tissue by TUNEL staining. Furthermore, PF4-Cre^{-} FasL$^{fl/fl}$ mice were used as control. Data are mean ± SEM (n = 6, 3 non-consecutive sections per animal were analyzed). *$P < .05$ for PF4-Cre^{+} animals treated with clodronate liposomes or control liposomes in comparison with PF4-Cre^{-} control animals. n.s., no significance.

eligible for thrombolysis therapy within a narrow time window after onset of symptoms.[65,66] Thus, to focus on the process of neuronal apoptosis in the penumbra, which lasts from hours to days after ischemia, could be a promising approach to modulate long-range tissue remodeling.[66,67] Understanding the mechanisms, how PLTs connect the initial events following vascular and tissue injury to restoration of tissue functionality, may provide feasible therapies for stroke or other diseases featuring PLT activation.

Acknowledgments

The authors thank Prof Andreas Strasser (The Walter and Eliza Hall Institute of Medical Research, Parkville, Victoria, Australia) for providing the FasL$^{\triangle m/\triangle m}$ mice, Prof Dr Martin-Villalba (University of Heidelberg) for providing the FasL$^{fl/fl}$ mice generated by Dr S. Karray (INSERM, France), and Sarah Gekeler and Birgit Fehrenbacher for excellent technical assistance.

This study was supported by the Volkswagen Foundation (Lichtenberg program), the German Heart Foundation, and Wilhelm Sander Foundation (H.F.L.). M.G. and H.F.L. are members of the Tuebingen Platelet Investigative Consortium funded by the German Research Council (Deutsche Forschungsgemeinschaft, KFO 274-PLTs: Basic mechanisms and clinical implications). F.R., F.T., and F.E. are supported by the Emmy Noether program of the Deutsche Forschungsgemeinschaft, the Else Kroener Fresenius Foundation, and the Excellence Initiative of the German Research Foundation (GSC-4, Spemann Graduate School). L.O. is supported by a National Health and Medical Research Council (Australia) project grant, National Health and Medical Research Council infrastructure grant, and the Victorian State Government (OIS grant).

Authorship

Contribution: R.I.S. designed and performed experiments, analyzed data, performed statistical analyses, and wrote the paper; F.R., F.T., A.K., M.O., M.S., I.H., and P.K. performed experiments and analyzed data; K.G. and S.G.M. performed experiments, analyzed data, and edited the paper; L.O., T.G., A.B., M.L., M.G., C.K.,

K.S.-O., S.W., X.L., M.S., and M.O. analyzed data and helped to conceptualize the project; F.E. designed experiments, performed experiments, analyzed data, and wrote the manuscript; and H.F.L. conceptualized the project, designed experiments, analyzed data, and wrote the paper.

Conflict-of-interest disclosure: The authors declare no competing financial interests.

Correspondence: Harald F. Langer, Section for Cardioimmunology, Eberhard Karls University Tuebingen, Otfried-Muller-Strasse 10, 72076 Tuebingen, Germany; e-mail: harald.langer@med.uni-tuebingen.de; and Frank Edlich, Institute for Biochemistry and Molecular Biology, ZBMZ, University of Freiburg, Stefan-Meier-Strasse 17, 79104 Freiburg, Germany; e-mail: frank.edlich@biochemie.uni-freiburg.de.

References

1. Wagner DD, Frenette PS. The vessel wall and its interactions. *Blood.* 2008;111(11):5271-5281.
2. Varga-Szabo D, Pleines I, Nieswandt B. Cell adhesion mechanisms in platelets. *Arterioscler Thromb Vasc Biol.* 2008;28(3):403-412.
3. Nachman RL, Rafii S. Platelets, petechiae, and preservation of the vascular wall. *N Engl J Med.* 2008;359(12):1261-1270.
4. Ruggeri ZM, Mendolicchio GL. Adhesion mechanisms in platelet function. *Circ Res.* 2007;100(12):1673-1685.
5. Gawaz M, Langer H, May AE. Platelets in inflammation and atherogenesis. *J Clin Invest.* 2005;115(12):3378-3384.
6. Stellos K, Kopf S, Paul A, et al. Platelets in regeneration. *Semin Thromb Hemost.* 2010;36(2):175-184.
7. Langer HF, Gawaz M. Platelets in regenerative medicine. *Basic Res Cardiol.* 2008;103(4):299-307.
8. Klinger MH, Jelkmann W. Role of blood platelets in infection and inflammation. *J Interferon Cytokine Res.* 2002;22(9):913-922.
9. Nieswandt B, Pleines I, Bender M. Platelet adhesion and activation mechanisms in arterial thrombosis and ischaemic stroke. *J Thromb Haemost.* 2011;9(suppl 1):92-104.
10. Jackson SP. Arterial thrombosis–insidious, unpredictable and deadly. *Nat Med.* 2011;17(11):1423-1436.
11. Langer HF, Gawaz M. Platelet-vessel wall interactions in atherosclerotic disease. *Thromb Haemost.* 2008;99(3):480-486.
12. Siddiqui TI, Kumar K S A, Dikshit DK. Platelets and atherothrombosis: causes, targets and treatments for thrombosis. *Curr Med Chem.* 2013;20(22):2779-2797.
13. Langer HF, Choi EY, Zhou H, et al. Platelets contribute to the pathogenesis of experimental autoimmune encephalomyelitis. *Circ Res.* 2012;110(9):1202-1210.
14. Boilard E, Nigrovic PA, Larabee K, et al. Platelets amplify inflammation in arthritis via collagen-dependent microparticle production. *Science.* 2010;327(5965):580-583.
15. Fuchs Y, Steller H. Programmed cell death in animal development and disease. *Cell.* 2011;147(4):742-758.
16. Green DR, Galluzzi L, Kroemer G. Mitochondria and the autophagy-inflammation-cell death axis in organismal aging. *Science.* 2011;333(6046):1109-1112.
17. Hotchkiss RS, Strasser A, McDunn JE, Swanson PE. Cell death. *N Engl J Med.* 2009;361(16):1570-1583.
18. Mc Guire C, Beyaert R, van Loo G. Death receptor signalling in central nervous system inflammation and demyelination. *Trends Neurosci.* 2011;34(12):619-628.
19. Walker NI, Harmon BV, Gobé GC, Kerr JF. Patterns of cell death. *Methods Achiev Exp Pathol.* 1988;13:18-54.
20. Youle RJ, Strasser A. The BCL-2 protein family: opposing activities that mediate cell death. *Nat Rev Mol Cell Biol.* 2008;9(1):47-59.
21. Eskes R, Antonsson B, Osen-Sand A, et al. Bax-induced cytochrome C release from mitochondria is independent of the permeability transition pore but highly dependent on Mg2+ ions. *J Cell Biol.* 1998;143(1):217-224.
22. Annis MG, Soucie EL, Dlugosz PJ, et al. Bax forms multispanning monomers that oligomerize to permeabilize membranes during apoptosis. *EMBO J.* 2005;24(12):2096-2103.
23. Edlich F, Banerjee S, Suzuki M, et al. Bcl-x(L) retrotranslocates Bax from the mitochondria into the cytosol. *Cell.* 2011;145(1):104-116.
24. Llambi F, Moldoveanu T, Tait SW, et al. A unified model of mammalian BCL-2 protein family interactions at the mitochondria. *Mol Cell.* 2011;44(4):517-531.
25. Siegel RM, Frederiksen JK, Zacharias DA, et al. Fas preassociation required for apoptosis signaling and dominant inhibition by pathogenic mutations. *Science.* 2000;288(5475):2354-2357.
26. Aggarwal BB. Signalling pathways of the TNF superfamily: a double-edged sword. *Nat Rev Immunol.* 2003;3(9):745-756.
27. Kaufmann T, Strasser A, Jost PJ. Fas death receptor signalling: roles of Bid and XIAP. *Cell Death Differ.* 2012;19(1):42-50.
28. O' Reilly LA, Tai L, Lee L, et al. Membrane-bound Fas ligand only is essential for Fas-induced apoptosis. *Nature.* 2009;461(7264):659-663.
29. Li H, Zhu H, Xu CJ, Yuan J. Cleavage of BID by caspase 8 mediates the mitochondrial damage in the Fas pathway of apoptosis. *Cell.* 1998;94(4):491-501.
30. Luo X, Budihardjo I, Zou H, Slaughter C, Wang X. Bid, a Bcl2 interacting protein, mediates cytochrome c release from mitochondria in response to activation of cell surface death receptors. *Cell.* 1998;94(4):481-490.
31. Ware J, Russell S, Ruggeri ZM. Generation and rescue of a murine model of platelet dysfunction: the Bernard-Soulier syndrome. *Proc Natl Acad Sci USA.* 2000;97(6):2803-2808.
32. Mabrouk I, Buart S, Hasmim M, et al. Prevention of autoimmunity and control of recall response to exogenous antigen by Fas death receptor ligand expression on T cells. *Immunity.* 2008;29(6):922-933.
33. Langer HF, Stellos K, Steingen C, et al. Platelet derived bFGF mediates vascular integrative mechanisms of mesenchymal stem cells in vitro. *J Mol Cell Cardiol.* 2009;47(2):315-325.
34. Lonsdorf AS, Krämer BF, Fahrleitner M, et al. Engagement of αIIbβ3 (GPIIb/IIIa) with αvβ3 integrin mediates interaction of melanoma cells with platelets: a connection to hematogenous metastasis. *J Biol Chem.* 2012;287(3):2168-2178.
35. Burkhart JM, Vaudel M, Gambaryan S, et al. The first comprehensive and quantitative analysis of human platelet protein composition allows the comparative analysis of structural and functional pathways. *Blood.* 2012;120(15):e73-e82.
36. Herrmann AM, Göbel K, Simon OJ, et al. Glatiramer acetate attenuates pro-inflammatory T cell responses but does not directly protect neurons from inflammatory cell death. *Am J Pathol.* 2010;177(6):3051-3060.
37. Langer HF, Chung KJ, Orlova VV, et al. Complement-mediated inhibition of neovascularization reveals a point of convergence between innate immunity and angiogenesis. *Blood.* 2010;116(22):4395-4403.
38. Stellos K, Sauter R, Fahrleitner M, et al. Binding of oxidized low-density lipoprotein on circulating platelets is increased in patients with acute coronary syndromes and induces platelet adhesion to vascular wall in vivo–brief report. *Arterioscler Thromb Vasc Biol.* 2012;32(8):2017-2020.
39. Shattil SJ, Cunningham M, Hoxie JA. Detection of activated platelets in whole blood using activation-dependent monoclonal antibodies and flow cytometry. *Blood.* 1987;70(1):307-315.
40. Scorrano L, Oakes SA, Opferman JT, et al. BAX and BAK regulation of endoplasmic reticulum Ca2+: a control point for apoptosis. *Science.* 2003;300(5616):135-139.
41. Li Y, Zhang F, Nagai N, et al. VEGF-B inhibits apoptosis via VEGFR-1-mediated suppression of the expression of BH3-only protein genes in mice and rats. *J Clin Invest.* 2008;118(3):913-923.
42. Kleinschnitz C, Kraft P, Dreykluft A, et al. Regulatory T cells are strong promoters of acute ischemic stroke in mice by inducing dysfunction of the cerebral microvasculature. *Blood.* 2013;121(4):679-691.
43. Kleinschnitz C, Pozgajova M, Pham M, Bendszus M, Nieswandt B, Stoll G. Targeting platelets in acute experimental stroke: impact of glycoprotein Ib, VI, and IIb/IIIa blockade on infarct size, functional outcome, and intracranial bleeding. *Circulation.* 2007;115(17):2323-2330.
44. Kraft P, Schwarz T, Göb E, et al. The phosphodiesterase-4 inhibitor rolipram protects from ischemic stroke in mice by reducing blood-brain-barrier damage, inflammation and thrombosis. *Exp Neurol.* 2013;247:80-90.
45. Langhauser F, Göb E, Kraft P, et al. Kininogen deficiency protects from ischemic neurodegeneration in mice by reducing thrombosis, blood-brain barrier damage, and inflammation. *Blood.* 2012;120(19):4082-4092.
46. Galluzzi L, Aaronson SA, Abrams J, et al. Guidelines for the use and interpretation of assays for monitoring cell death in higher eukaryotes. *Cell Death Differ.* 2009;16(8):1093-1107.
47. Ahmad R, Menezes J, Knafo L, Ahmad A. Activated human platelets express Fas-L and induce apoptosis in Fas-positive tumor cells. *J Leukoc Biol.* 2001;69(1):123-128.
48. Nagata S. Fas ligand-induced apoptosis. *Annu Rev Genet.* 1999;33:29-55.
49. Lindsten T, Ross AJ, King A, et al. The combined functions of proapoptotic Bcl-2 family members bak and bax are essential for normal development of multiple tissues. *Mol Cell.* 2000;6(6):1389-1399.

50. Rondina MT, Weyrich AS, Zimmerman GA. Platelets as cellular effectors of inflammation in vascular diseases. *Circ Res.* 2013;112(11): 1506-1519.

51. Srinivasula SM, Ahmad M, Fernandes-Alnemri T, Litwack G, Alnemri ES. Molecular ordering of the Fas-apoptotic pathway: the Fas/APO-1 protease Mch5 is a CrmA-inhibitable protease that activates multiple Ced-3/ICE-like cysteine proteases. *Proc Natl Acad Sci USA.* 1996;93(25): 14486-14491.

52. Huang DC, Hahne M, Schroeter M, et al. Activation of Fas by FasL induces apoptosis by a mechanism that cannot be blocked by Bcl-2 or Bcl-x(L). *Proc Natl Acad Sci USA.* 1999;96(26): 14871-14876.

53. Hohlbaum AM, Moe S, Marshak-Rothstein A. Opposing effects of transmembrane and soluble Fas ligand expression on inflammation and tumor cell survival. *J Exp Med.* 2000;191(7):1209-1220.

54. Cullen SP, Henry CM, Kearney CJ, et al. Fas/CD95-induced chemokines can serve as "find-me" signals for apoptotic cells. *Mol Cell.* 2013; 49(6):1034-1048.

55. Spencer SL, Gaudet S, Albeck JG, Burke JM, Sorger PK. Non-genetic origins of cell-to-cell variability in TRAIL-induced apoptosis. *Nature.* 2009;459(7245):428-432.

56. Kraft P, Göb E, Schuhmann MK, et al. FTY720 ameliorates acute ischemic stroke in mice by reducing thrombo-inflammation but not by direct neuroprotection. *Stroke.* 2013;44(11):3202-3210.

57. Griffith TS, Brunner T, Fletcher SM, Green DR, Ferguson TA. Fas ligand-induced apoptosis as a mechanism of immune privilege. *Science.* 1995; 270(5239):1189-1192.

58. Semple JW. Platelets play a direct role in sepsis-associated endothelial cell death. *Thromb Haemost.* 2008;99(2):249.

59. Kuckleburg CJ, Tiwari R, Czuprynski CJ. Endothelial cell apoptosis induced by bacteria-activated platelets requires caspase-8 and -9 and generation of reactive oxygen species. *Thromb Haemost.* 2008;99(2):363-372.

60. Arabanian LS, Kujawski S, Habermann I, Ehninger G, Kiani A. Regulation of fas/fas ligand-mediated apoptosis by nuclear factor of activated T cells in megakaryocytes. *Br J Haematol.* 2012; 156(4):523-534.

61. Langer HF, May AE, Vestweber D, De Boer HC, Hatzopoulos AK, Gawaz M. Platelet-induced differentiation of endothelial progenitor cells. *Semin Thromb Hemost.* 2007;33(2):136-143.

62. Galluzzi L, Kepp O, Trojel-Hansen C, Kroemer G. Mitochondrial control of cellular life, stress, and death. *Circ Res.* 2012;111(9):1198-1207.

63. Youle RJ, van der Bliek AM. Mitochondrial fission, fusion, and stress. *Science.* 2012;337(6098): 1062-1065.

64. Clark SR, Ma AC, Tavener SA, et al. Platelet TLR4 activates neutrophil extracellular traps to ensnare bacteria in septic blood. *Nat Med.* 2007; 13(4):463-469.

65. Vosler PS, Chen J. Potential molecular targets for translational stroke research. *Stroke.* 2009; 40(3 suppl):S119-S120.

66. Lo EH, Dalkara T, Moskowitz MA. Mechanisms, challenges and opportunities in stroke. *Nat Rev Neurosci.* 2003;4(5):399-415.

67. Tymianski M. Emerging mechanisms of disrupted cellular signaling in brain ischemia. *Nat Neurosci.* 2011;14(11):1369-1373.

2015 126: 1483-1493
doi:10.1182/blood-2013-12-544445 originally published online July 31, 2015

Platelets induce apoptosis via membrane-bound FasL

Rebecca I. Schleicher, Frank Reichenbach, Peter Kraft, Anil Kumar, Mario Lescan, Franziska Todt, Kerstin Göbel, Ingo Hilgendorf, Tobias Geisler, Axel Bauer, Marcus Olbrich, Martin Schaller, Sebastian Wesselborg, Lorraine O'Reilly, Sven G. Meuth, Klaus Schulze-Osthoff, Meinrad Gawaz, Xuri Li, Christoph Kleinschnitz, Frank Edlich and Harald F. Langer

Blood (print ISSN 0006-4971, online ISSN 1528-0020), is published weekly by the American Society of Hematology, 2021 L St, NW, Suite 900, Washington DC 20036.